# Spatio-temporal variability of the Thermohaline and Biogeochemical properties and Dissolved Organic Carbon in a coastal embayment affected by upwelling: the Ría de Vigo (NW Spain).

---

M. D. Doval*, E. Nogueira, Fiz F. Pérez

*Instituto de Investigacións Mariñas, C.S.I.C. Eduardo Cabello, 6. 36208 Vigo, Spain.*

*Corresponding author. Fax number: 34-86-292762. E-mail: marylo@iim.csic.es

**Abstract**

Hydrographic sampling was carried out along the main axis of the Ria de Vigo, from May 1994 to September 1995, to observe the spatio-temporal evolution of hydrographic and biogeochemical properties of the water column. Meteorology controls mainly the hydrography and biogeochemistry of the Ría. Two periods can be distinguished on a seasonal-time-scale: the upwelling season, from March to October and the non-upwelling season, from November to February. A strong coupling was observed between meteorological, hydrographic and biogeochemical processes. The ría behaves like an extension of the shelf during the upwelling season and like a partially mixed estuary during the non-upwelling season.

Dissolved organic carbon was related to the thermohaline properties in the whole water column, and with oxygen and chlorophyll *a* in the surface layer. Extreme values were recorded during the upwelling season: the highest values (>100 µM), in the surface layer during upwelling relaxations and the lowest values (<70 µM), in the bottom layer in upwelled waters. Dissolved organic carbon maxima decrease shelfwards thus suggesting export of dissolved organic carbon, in addition to particulate organic carbon, from the ría to the shelf.

KEYWORDS: upwelling, non-upwelling, hydrography, biogeochemical, DOC, Ría de Vigo (NW Spain).

## 1. Introduction

The Galician Rias Baixas are four coastal embayments in the NW Iberian Peninsula, occupying the northern boundary (42º to 43ºN) of the NW Africa upwelling system, which extends from 10º to 44ºN (Wooster et al., 1976). At a seasonal time-

scale, the main hydrographic features along the Galician coast of the Iberian Peninsula are closely related to the large-scale climatology of the northeast Atlantic (Blanton et al., 1987; Haynes et al., 1993). From April to October, mainly during the summer, with the onset of the summer Portuguese trades, the Azores high pressure cell is located in the central North Atlantic, and the Greenland low pressure has diminished in intensity. The resulting atmospheric pressure field forces northerly winds along the Galician coast, and thus, it induces coastal upwelling. The prevailing northerly winds produce a 1 to 2 weeks stress/relaxation cycle (Blanton et al., 1987), which is the main controller of estuarine circulation (Álvarez-Salgado et al. 1996a; 1996b). Upwelling lifts the cold, nutrient-rich Eastern North Atlantic Central Water (ENACW) from 150 to 200m depth to above 50m (Álvarez-Salgado et al., 1993), shallow enough to enter the rias by means of the enhanced residual circulation.

By contrast, the rest of the year, mostly during the winter, the Azores high pressure cell is located off the northwestern Africa coast and it has diminished in intensity, whereas the Greenland low pressure is deepened and located off the southeastern coast of Greenland. The atmospheric pressure field results in an onshore wind with a strong southerly component. Southerly winds, generate downwelling, thus forcing shelf surface waters to move towards the rias. In this situation, the balance between river discharge and shelf wind stress will ultimately determine the flow of water, giving rise to a reversal in the positive circulation during strong downwelling events (Álvarez-Salgado et al., 1996a).

Dissolved organic matter (DOM) has been historically ignored because it was considered biologically inert. Despite that, dissolved organic carbon (DOC) is the major reservoir of organic carbon in the oceans. The new HTCO (High temperature catalytic oxidation) method allows the detection of small but real differences in the bulk DOC

mediated by biogeochemical processes. (Kirchman et al., 1993; Cauwet, 1994). Thus the inclusion of DOM in biogeochemical models is essential. However, little is known about the absolute concentration, characterisation and transformation of DOM in seawater (Sharp et al., 1993).

Ocean margins are a key area for investigating the global impact of DOC on the carbon cycle (Wollast, 1991), since both the export of terrestrial DOC and the import of oceanic DOC occur at this boundary. There are profound implications for mass-balancing carbon budgets and material fluxes across estuarine and shelf interfaces and within oceanic systems (Jackson, 1988).

The ria de Vigo has recently been the subject of several hydrographic studies mainly during the upwelling season (Ríos, 1992; Prego 1993a; 1993b; 1994; Figueiras et al., 1994; Gómez-Fermin et al., 1996). They report several aspects on hydrography, general estuarine circulation, nutrients and plankton response, in relation to upwelling events. However, none of these surveys evaluate the interrelation and coupling between meteorological, thermohaline and biogeochemical variables along the upwelling and non-upwelling seasons and the spatio-temporal evolution of DOC and $pCO_2$ (partial pressure of carbon dioxide) in this Ria.

## 2. Materials and methods

### *2.1. Survey area and sampling*

The Ria de Vigo (Fig 1) penetrates on the Galicia coast of the Iberian Peninsula following approximately a north-east direction. The Ria de Vigo is located between 42º 07’ and 42º 21’N, 8º 36’ and 8º 54’W; it is the most meridional of the Rías Baixas. The surface:volume ratio is 0.05, typical of v-shaped basin systems that gradually deepen and widen towards the mouth, thus favouring export (Odum et al., 1979).

Two areas can be distinguished, in accordance with the degree of continental and oceanic influences. The innermost zone, San Simón bay, behaves as a typical estuary, due to the effects of tides (average tidal range, 3 m) and to the direct influence of the Oitaben-Verdugo river discharge (Pérez et al, 1992). This river is the main tributary to the Ría de Vigo, with a mean annual flow of 13 $m^3$ $s^{-1}$ (Ríos et al., 1992a). The outermost zone, directly influenced by the ocean endmember, includes the area between Cabo de Mar and the Cíes islands. Station 1 (Fig. 1), placed over the main channel (45 m depth) in the central part of the ria (42º 14.5´N, 8º 45.8´W), is affected by both continental and ocean waters. It is a 'time-series' station sampled twice a week from 1987. Station 2, (90 m depth), situated off the Ría (42º 08.5´N, 8º 57.5´W) is under oceanic influence. They were the representative stations chosen for describing the time evolution of the hydrographic conditions along the period studied.

Hydrographic sampling for these two stations was carried out twice a month in the Ria de Vigo (Fig. 1), from May 5, 1994 to September 21, 1995. The mean flushing time for the ria de Vigo, estimated using a box model approach (Prego and Fraga, 1992; Ríos, 1992), is about a fortnight. The sampling interval is similar to this mean flushing time. Water samples were drawn from 3 to 8 depths (depending on the bathymetry) with 5l Niskin bottles. Date for each radial transect is shown in Table 1. Figures 3 to 8 (except 7) has been obtained using a Surfer mapping system, 6.3. The minimum curvature was used as interpolating method.

*2.2. Meteorological properties.*

The upwelling index is an estimation of the flow of upwelled seawater per km of coast (Ekman transport). According to Bakun (1973):

$$I_w = 1000 \frac{C_d \rho_a \left|\vec{V}\right|}{f\rho_w} . V_N \ (m^3 s^{-1} km^{-1})$$

where $C_d$ is an empirical drag coefficient, equal to $1.4 \times 10^{-3}$ (dimensionless); $\rho_a$ is the air density, equal to 1.2 kg·m$^{-3}$; $V$ is the wind speed in m·s$^{-1}$; $V_N$ is the north component of wind; $\rho_w$ is the seawater density, equal to 1026 kg m$^{-3}$; and $f$ is the Coriolis parameter, equal to $9.9 \times 10^{-5}$ s$^{-1}$ at 43º latitude. The upwelling index was calculated at 43ºN, 11ºW (150 km off Cape Finisterre) using geostrophic winds deduced from surface pressure charts, provided 3 times per day. Positive values indicate upwelling and negative values indicate downwelling. Runoff in the drainage basin (590 km$^2$) was estimated as a function of precipitation by using the equation given by Ríos et al (1992). The incoming solar radiation, Qs, was estimated by Mosby`s formula (Dietrich et al., 1980). The meteorological values showed (Fig 2 a, b and c) result from averaging the daily values from the current date to four days before. The reason for this is based on the inertia of coastal circulation to wind stress (McClain et al., 1986; Rosón et al., 1997).

*2.3. Thermohaline properties.*

Temperature and salinity were recorded by means of a CTD (25-01 SBE) probe. Temperature was determined with a precision of ±0.004ºC, and salinity with ±0.003 PSS determined from conductivity measurements using the equation proposed by UNESCO (1991). discrete samples of salinity were collected and analysed with an AUTOSAL 8400 A to calibrate the conductimeter of the CTD probe

*2.4. Biogeochemical properties.*

Nutrients samples were collected on solid PVC containers and frozen to -20 ºC until analysis in the laboratory with an Alpkem ® segmented flow analysis (SFA)

system. The precision (analytical error determined with standard replicates) was ± 0.02 µmol $kg^{-1}$ for nitrite, ± 0.05 µmol $kg^{-1}$ for nitrate, ± 0.1 µmol $kg^{-1}$ for ammonium, ± 0.2 µmol $kg^{-1}$ for silicate and ± 0.01 µmol $kg^{-1}$ for phosphate. Oxygen was determined by Winkler potentiometric titration (Culberson, 1981). The precision was ±0.5 µmol $kg^{-1}$ and the analyzer used was a Titrino 720 (Metrhom). pH (NBS) was measured potentiometrically according to Pérez and and Fraga (1987a). Alkalinity was determined by acid titration to pH 4.4 following Pérez and and Fraga (1987b). The precision were ±0.005 for pH and ±2.5 µmol.$kg^{-1}$ for alkalinity. The $pCO_2$ was determined substituting pH and the alkalinity in the carbonic acid system equations, using the constants proposed by Mehrbach et al. (1973) and Weiss (1974) in agreement with Takahashi et al. (1993). The precision was ±5 µatm. Chlorophyll *a* was measured fluorometrically, using a Turner Design 10000 R fluorometer, after 90% acetone extraction (Yentsch and Menzel, 1963). The precision was ±0.05 µg.$l^{-1}$.

*2.5. Dissolved organic carbon.*

DOC determination was performed by high temperature catalytic oxidation (HTCO), with a commercial 'Shimadzu TOC-5000'. The combustion quartz tube was filled with a 0.5% Pt on $Al_2O_3$ catalyst. Three to 5 replicate injections of 200 µl were performed per sample. The concentration of DOC was determined by subtracting the average peak area from the instrument blank area and dividing by the slope of the standard curve (Thomas et al., 1995). The instrument blank is the system blank plus the filtration blank. The system blank was determined by subtracting the DOC in UV-Milli-Q to the total blank. Measurements made with the high sensitivity catalysts (Pt on silica wool) produced values <2 µM-C for fresh UV-Milli-Q water. The filtration blank was

determined by filtering UV-Milli-Q water through the filtration system. The filtration blank was ~5 µM-C. Before sample analyses, the catalyst was washed by injecting samples of UV-Milli-Q, for at least 12 h, until the system blank was low and stable. The system blank is <8 µM-C; when it was higher, we washed or even replaced the catalyst. The system was standardised with Potassium Hydrogen Phthalate (KHP). The coefficient of variation of the peak area for the 3-5 replicates of each sample was ~1-2 %, i.e., the precision can be estimated as about 1 to 3 µM.

## 3. Results and discussion

### *3.1. Wind patterns*

The wind-featured seasons in the NW Iberian upwelling system can be easily identified from the time-course of Iw (Fig. 2a). Two wind-featured seasons could be observed, closely related to the large-scale wind climatology of the subtropical gyres: an upwelling season, from March to October and a non-upwelling season, from November to February (Table 1). The N-NE and N-NW winds were the most favourable for the coastal upwelling into the ría. The S-SW winds were predominant during the non-upwelling season (Nogueira et al., 1997). Short-time-scale fluctuations over the seasonal pattern occur: brief events of upwelling favourable winds are occasionally perceptible during the winter (Fig. 2a: January'95, R17), as well as downwelling favourable winds are perceived during the upwelling season (Fig. 2a: May ,R1; August, R6-R7; and September, R9-R10, in the year ´94, and May, R24; July, R26-R29 and September, R33 in the year `95). In addition, transient conditions between both wind-featured seasons are also quite singular. The change from the upwelling to the downwelling season, the 'fall transition' (Fig. 2a, September-October ´94, R11-R12) and the change from the downwelling to the upwelling season, the 'spring transition' (Fig. 2a, March 95, R21-

R22), are both marked by drastic changes on the meteorological conditions, specially of winds.

The aforesaid features could be clearly distinguished in Table 2, where some statistics of the cross-shore Ekman transport in the sampling period are shown. The statistics are given for the wind-featured seasons as well as for the astronomic seasons in order to point out the greater variability observed during the fall and spring transitions.

Thus, at the seasonal time-scale, the large-scale wind climatology controls the local meteorology in the Galician coast, which in turn will influence both the hydrodynamic and the biogeochemical behaviour of the rías. We will show this tightly coupling for the Ría de Vigo.

### *3.2. Hydrographic response*

#### *Upwelling season*

In the study period, two upwelling seasons were sampled: from May to October 1994 (R1 to R12) and from March to September 1995 (R21 to R34), (Table 1). Spring and fall transitions were included in upwelling season.

They were characterised by intermittent northerly winds which cause a succession of upwelling-relaxation events, with a periodicity of 7 to 14 days (Fig 2a, Table 2). During both periods, runoff to the ría was limited, although episodes of variable intensity and duration do occasionally occurred (Fig. 2b, May ´94, R1-R2 and May ´95, R25-R26), and irradiance generally exceeded 500 $cal \cdot cm^{-2} \cdot day^{-1}$ (Fig. 2c).

During the upwelling season, northerly winds promote the upwelling of Eastern North Atlantic Central Water (ENACW) over the shelf and its displacement along the bottom into the Ria (Fraga, 1981; Álvarez-Salgado et al., 1993). The response of the system to the upwelling-relaxation cycles could be appreciated in the peaks and thoughts

of the 13°C isotherm (*ca*., the upper limit of ENACW), (Figs. 3a, 4a). Main upwelling events were around June (R3), July (R6) and September (R10) 1994, and March (R22), April (R24), June (R27), August (R31-32) and September (R34) 1995. Since there is a linear relationship between salinity and temperature of ENACW (Ríos et al., 1992b), the signature of the upwelling-relaxation cycles could be also observed in the time-course of salinity (Figs. 3b, 4b). Since the water budget is negative (River (R) + Precipitation (P) < Evaporation (E)), stratification is mainly of thermal origin, being maximum thermal gradient centred in July (Figs. 3a, 4a, around R4 in the year '94 and R30 in the year '95). However, episodic freshwater inputs contribute to enhance water-column stability by haline stratification (Figs. 3b, 4b: May ´94, R2 and May and July ´95, R26, R30). On the other hand, during strong upwelling events the bottom water may reach the surface (Figs. 2b, 3b: September ´94, R10 and August ´95, R32) and then, the stratification is broken.

The most obvious chemical feature of an upwelling event is the higher level of inorganic nutrient salts in the bottom layer, mainly $NO_3^-$, $Si(OH)_4$ and $HPO_4^{2-}$. The intermittent intrusion of nutrient rich ENACW could be appreciated in the sloping up of the isolines of $NO_3^-$ (Figs 3c, 4c), $Si(OH)_4$ (Figs. 3d, 4d) and $pCO_2$ (Figs. 5c, 6c) and the sloping down of the isolines of $O_2$ (Figs. 5b, 6b) when upwelling-favourable northerly winds occur (Fig. 2a). Concentrations between 9 to 12 µmol $kg^{-1}$ $NO_3^-$, 7 to 11 µmol $kg^{-1}$ $Si(OH)_4$ and 400 to 600 µatm $pCO_2$ and minimum $O_2$ concentration between 200 to 150 µmol $kg^{-1}$, were measured at the bottom layer due to the advection of upwelled waters aged on the shelf and into the ría. Nutrient replenishment in the surface layer is mediated by strong upwelling pulses or episodic runoff events. However, nutrients advected from runoff were quickly consumed in the inner ría as showed the lower values observed during this season.

*Non-upwelling season*

This season, from November‘94 to February’95 (R13-R20), (Table 1) is characterised by the prevalence of southerly and southwesterly winds, causing strong downwelling events, with a periodicity of *ca*. 24 days (Fig 2, Table 2). During this period, runoff to the Ria (which is related with the prevailing wind pattern (Fig 2c)) was large -the most intense episode taking place by November ‘94 (R13-R14) and January-February ‘95 (R17-R20)-, and irradiance was low, about 250 cal. $cm^{-2}$ $day^{-1}$ (Fig 2c).

The hydrographic behaviour of the Ria is controlled mainly by runoff and downwelling events, both associated with southerly and southwesterly winds. Downwelling events can be recognised by the downward displacement of the 13ºC isotherm and 35.7 isohaline (Figs 3a, 4a and 3b, 4b). Larger runoff episodes can be identified by the low salinity levels (Fig 3b, 4b) in surface waters, enhancing the haline stratification and thus the stabilisation of the water column. On the other hand, the advection of warm shelf surface water (16ºC) provokes thermal inversion at station 2 and thermal homogenisation at station 1 between November 1994 and January 1995 (R13-R17).

The most obvious chemical feature of a downwelling event was the drastic change of inorganic nutrient salts in the water column, with sloping down of the isoline of $NO_3^-$ (Figs 3c, 4c), $Si(OH)_4$ (Figs 3d, 4d) and $pCO_2$ (Figs.5c, 6c) and sloping up of the isoline of $O_2$ (Figs. 5b, 6b) at the bottom layer. In bottom waters, nutrient concentrations were low except when an anomalous upwelling event occurred during January ‘95 (R17). In the surface layer, mixing of nutrient-rich continental waters and shelf waters that enters into the ria, characterised nutrient distributions in the surface layer. For a high runoff episode, the most strickling chemical feature was an increased

level of $NO_3^-$ (Figs 3c, 4c) and specially $Si(OH)_4$ (Figs 3d, 4d), (the main tracer of continental inputs due to the litological character of the drainage basin) with maximum of >10.5 $NO_3^-$ and >13 µmol.kg$^{-1}$ $Si(OH)_4$ between January-February '95 (R18-R20) on station 1. During this period, nutrients were higher in the upper layer than in the lower layer.

The main hydrographic difference between both stations was that, whereas station 1 showed higher haline and thermal stratification, since it is more influenced by runoff, station 2 showed more markedly oceanic influences due to the presence of ENACW waters at the bottom layer in nearly all the period studied. The Temperature/Salinity distribution in the salinity maximum (Fig. 7) clearly showed these differences.

*3.3. Biogeochemical response*

*Chlorophyll a distribution*

At the time-scale of this study, the factors which control phytoplankton biomass dynamics are the seasonal variation of incoming solar radiation, advection -or circulation-, stability and nutrients (Legendre, 1981).

The chlorophyll *a* (Chl *a*) concentration can be considered as a estimation of phytoplankton biomass. Chl *a* maxima (Fig.5d, 6d) appear during upwelling relaxations, when the system have enough nutrients and the water exchange with the shelf is not very high (Rosón et al., 1995).

During the upwelling season, the distribution showed two main peaks: the Spring and Autumn blooms. The Spring bloom was detected on March ´95 (R22), (Chl *a*: >7 µg.l$^{-1}$, $O_2$: >330 µmol.kg$^{-1}$) at station 1. This bloom was developed under hydrodynamic control, due to moderate upwelling (R21) that preceded the slow

estuarine circulation supposed in the moment of the bloom. Autumn blooms were found at the end of the two upwelling seasons studied; only at station 2 in 1994 (Chl *a*: >9 $\mu g.l^{-1}$, $O_2$ >280 $\mu mol.kg^{-1}$) and at both sampling stations in 1995 (Chl *a* >5 $\mu g.l^{-1}$, $O_2$ >240 $\mu mol.kg^{-1}$). During this season, other maxima of Chl *a* and $O_2$ were measured: May ´94 (R2) and May´95 (R27), that were due to moderate upwelling nutrient replenishment by a little runoff event (Fig.2b).

During the non-upwelling season, primary production was light limited (Fig. 2c, Qs ≈250 $cal.cm^{-2}.day^{-1}$). It is however noticeable the winter bloom (Chl *a*>3 $\mu g.l^{-1}$) developed at surface of station 1 (December '94, R15) during calm winds conditions.

*Biogeochemical variables distribution*

The biogeochemical variables considered ($NO_3^-$, $NH_4^+$, $O_2$, $pCO_2$ and Chl *a*), are strongly influenced in the upper layer by photosynthetic activity of phytoplankton, by inflow of continental inputs and by upwelled waters. In the bottom layer, the succession of upwelling-downwelling events and the remineralisation processes can explain the observed variability.

In agreement with the photosynthesis-remineralisation processes, nutrients and $pCO_2$ decreased when Chl *a* and $O_2$ increased in the surface layer. However, when nutrient and $CO_2$ rich-upwelled waters outcrop the surface, high $NO_3^-$ and $pCO_2$ concentrations were observed coinciding with high Chl *a* values. $pCO_2$ has a more conservative behaviour than Chl *a* due to sedimentation and grazing of phytoplankton. Therefore, $pCO_2$ and Chl *a* were uncoupled in the surface layer. These processes can be followed from the distributions of $NO_3^-$ (Fig 3c, 4c), $O_2$ (Fig. 5b, 6b), $pCO_2$ (Fig. 5c, 6c) and Chl *a* (Fig.5d, 6d).

The variation of chemical properties in the deep layer was obviously tied to the variability of thermohaline properties. (Fig. 3a, 4a, 3b and 4b). Coupling between water displacements and nitrate (Fig. 3c, 4c), oxygen (Fig. 5b, 6b) and $pCO_2$ (Fig. 5c, 6c) levels in the lower layer could be observed in the time course of the 5 to 9 µmol.kg$^{-1}$ isolines of nitrate, the 230 to 180 µmol.kg$^{-1}$ isolines of oxygen, and the 440 to 540 µatm isolines of $pCO_2$ regarding the 13ºC isotherm and the 35.7 isohaline. The aforesaid chemical features of upwelled water were accentuated by mineralisation processes of organic matter exported from the ria, that take place over the shelf (Tenore et al.,1982; López Jamar et al., 1992). The concentrations of $NO_3^-$ and $pCO_2$ showed a small increase in time from May to October ´94 (9 to 11,12 µmol.kg$^{-1}$) and from March to September ´95 (9 to 13 µmol.kg$^{-1}$) in agreement with Alvarez-Salgado et al. (1993).

As previously mentioned, during the upwelling season, (May-October '94, March-September '95), (Table 1) the inward flow of ENACW brings nitrate to the lower layers. On the other hand, the high Chl *a* and oxygen levels at the upper layers, coinciding with upwelling relaxations showed higher phytoplankton biomass. The pelagic and benthic remineralisation processes and sediment water exchange were more evident during the relaxation and moderate downwelling events, as they produced a sloping up in nutrients and $pCO_2$ isolines: high levels of $pCO_2$ and nitrate were observed in September (R8-R10) at station 1, >600 µatm and >11 µmol kg$^{-1}$ and in November (R13-R14) at station 2, >600 µatm and >12 µmol kg$^{-1}$, respectively. The sequence: production-sedimentation-regeneration can be followed with the distributions of Chl *a* and $NH_4^+$. After Chl *a* maxima, $NH_4^+$ maxima were measured, coinciding with relaxation periods. On the other hand, higher $NH_4^+$ levels in summer could be due to more stratified conditions in summer than in spring. Therefore, nutrient inputs to the ria

are supplied by subsurface oceanic water and by remineralisation processes inside the ria, about 70% and 25% respectively in summer (Prego, 1994).

During the non-upwelling season (November '94-February '95) (Table 1), $NH_4^+$ maximum was found at both layers in November, due to advection of waters regenerated in the innermost part of estuary (Pérez et al., 1992) and ammonium diffused from the sediments (Álvarez-Salgado et al., 1996a,b). High $NO_3^-$ and $pCO_2$ peaks were showed too on November, at surface of station 1 (>6 and >450 µmol.kg$^{-1}$, respectively). These maxima coincides with the temperature maxima (Fig. 3a, 4a) at downwelling events, when water circulation is blocked. However, $NO_3^-$ diminished below 1 µmol kg$^{-1}$ at surface of station 2. The highest $NO_3^-$ at both stations were sampled in January due to the strong freshwater influence. As showed before, during this period, nutrients were higher in the upper layer than the lower layer, because the influx of nutrients by runoff, but photosynthesis was serious limited by light (Fig. 2c) and advected nutrients were not uptaked.

In summary, the remineralisation process include pelagic and benthic remineralisation over the shelf and at the different parts of the ria. The relative high levels of nitrite and specially of ammonium in this ría (the mean value of $NO_2^-$: 0.2, $NH_4^+$: 1.1 and $NO_3^-$: 5.2 µmol kg$^{-1}$, n: 670 samples) affect the Redfield ratio ($-O_2$/DIN) of oxygen consumption to DIN (dissolved inorganic nitrogen). Therefore, we use the oxygen correction ($O_2$ cor = $O_2$ - 0.5 $NO_2^-$ - 2 $NH_4^+$), introduced by Ríos et al. (1989) and Fraga et al. (1992), since 0.5 mole of oxygen is necessary to oxidise 1 mole of nitrite to nitrate, and 2 moles of oxygen is necessary to oxide 1 mole of ammonium to nitrate. The relation between AOUc (AOUc = $O_2$ sat - $O_2$ cor) and DIN for all the samples (n: 670, $r^2$~ 0.7) was: AOU: -49 (±25) + 10.4 (±0.3) DIN. This relation, obtained minimising the area $\sum_i(AOU_i - AOU_m)\cdot(DIN_i - DIN_m)$, being $AOU_m$ and $DIN_m$

the average values of AOU and DIN respectively, are in agreement with the regulation by cyclical production-remineralisation of nutrients in the Ria de Arosa (Álvarez-Salgado et al., 1996a). The slope obtained for this relation (10.4) in the Ría de Vigo was similar to the Redfield ratio (Rn: 9.5) calculated in the open ocean. On the other hand, the coefficient of correlation ($r^2$ ~0.7) was not higher due to variation in the Rn value, and losses of $O_2$ to the atmosphere.

*DOC distribution.*

The distribution of DOC (Fig. 8a, 8b) was similar to that of temperature (Fig. 3a, 4a) and salinity (Fig. 3b, 4b); isolines of DOC were sloping up with the advection of ENACW at both stations. During the upwelling season, the isolines between 60 and 80 µM-C point out the succession of upwelling-downwelling events. During the non-upwelling season, the reversal in circulation occurred by October provoked homogeneatization of DOC and a subsurface maximum of 110 µM-C at 15 m of station 1.

At surface, the distribution of DOC was coupled to the distribution of $O_2$ (Fig. 5b, 6b) and Chl *a* (Fig. 5d, 6d), that showed high levels during upwelling relaxations periods. However, DOC did not show high levels during the Spring bloom at March ´95 (R22), with high levels of Chl *a* and $O_2$, at station 1.

All profiles showed significant decrease of DOC with depth. The maxima range were 150-56 µM at station 1 and 130-53 µM at station 2. The mean values of DOC were: 106 and 95 µM at surface of station 1 and 2, respectively, and 77 and 67 µM at bottom layer of station 1 (45m) and 2 (90 m), respectively. It was evident the higher concentration of DOC at the most internal station (station 1). On the other hand, the relative high mean DOC at surface of station 2 and shelf waters off the Ría de Vigo (42º

7.8'N, 9º 7.5'W; Doval M.D., unpubl. data), 95 and 82 µM, respectively, confirm the export of DOC from the rias to the shelf, in addition to the Particulate Organic Matter (POM) suggested by other authors (Fraga, 1981; Alvarez-Salgado et al., 1993).

Our DOC values were in the same range as those recently reported by several authors (Cauwet et al., 1990, 1994; Tupas et al., 1994; Thomas et al., 1995). In the North Atlantic, we have measured (Doval et al., 1997 and Doval M.D. unpubl. data) values, between 40 and 43ºN, ranging 50-100µM with average maximum of 90 at surface and average minimum of 55 at depth higher than 1000 m.

## 4. Summary and Conclusions

The evolution and distribution of hydrographic and biogeochemical properties in the Ria de Vigo is controlled mainly by the variability of meteorological properties that allow us to distinguish, at a seasonal time scale, two wind-featured seasons: the upwelling season, from March to October and the non-upwelling season, from November to February. A tightly coupling was observed between meteorology, hydrodynamic and biogeochemical processes. The ria behaves like an extension of the shelf during the upwelling season and like a partially mixed estuary during the non-upwelling season.

Biogeochemical processes, like the development of the chlorophyll *a* bloom, production-remineralisation sequence, and the diffusion from the sediments are clearly under hydrodynamic control. In this study we also showed the role played by the inner part of the ria in the modification of the continental inputs by remineralising the organic material and by increasing the production by nutrient replenishment events from river input .

Our results demonstrated that the HTCO method can generate reliable, rapid and precise DOC, which allows the detection of small, but real differences in the bulk DOC stocks. DOC distribution is coupled with the thermohaline properties through the water column and with $O_2$ and Chl *a* in the surface layer. Extreme values were registered during the upwelling season: the highest DOC in the surface layer at relaxation periods, and the lowest DOC, in the bottom layers in upwelled waters. DOC maxima decrease from the inner to the outer stations of the ría, thus suggesting export of dissolved organic carbon from the ría to the shelf. If DOC is a major form of carbon export from the upper ocean (Carlson et al., 1994), DOC would be the major organic material export from the Ria de Vigo surface waters. Although, the relative importance of this export depends largely on the production and consumption processes of the system (Carlson et al., 1995).

**Acknowledgments**

We thank the members of the group of oceanography from the Instituto de Investigacións Mariñas of Vigo, who participate in the surveys and the crew of the Jose Mª Navaz for their help. We also thanks R. Penín and M. V. González for the analysis of particulate organic matter, chlorophyll-*a* and sample filtration; T. Rellán for the analysis of carbon system variables and M. J. Pazó for nutrient analysis. A fellowship from the EC MAST project CT93-0065 allowed M.D. Doval and E. Nogueira to carry out this work. This work was financed in part by the Comisión Interministerial de Ciencia y Tecnología (CICYT) under proyect AMB92-0165. We also thank Dr. F. Fraga and Dr X. A. Álvarez-Salgado for their valuable comments.

**References**

Álvarez-Salgado, X. A., Rosón, G., Pérez, F. F. and Pazos, Y. 1993 Hydrographic variability off the Rías Baixas (NW Spain) during the upwelling season. J. Geophy Res 98 (C8): 14447-14455

Álvarez-Salgado, X. A., Rosón, G., Pérez, F. F., Figueiras, F. G. and Pazos, Y. 1996a Nitrogen cycling in an estuarine upwelling system, the Ría de Arousa (NW Spain). I. Short-time-scale patterns of hydrodynamic and biogeochemical circulation. Mar Ecol Prog Ser 135: 259-273

Álvarez-Salgado, X. A., Rosón, G., Pérez, F. F., Figueiras, F. G. & Ríos, A. F. 1996b Nitrogen cycling in an estuarine upwelling system, the Ria de Arosa (NW Spain). II. Spatial differences in the short-time-scale evolution of fluxes and net budgets. Mar Ecol Prog Ser 135: 275-288.

Bakun, A. 1973 Coastal upwelling indices, west coast of North America, 1946-71, NOAA, Tech. Rep., NMFSSSRF-671, 103 pp.

Blanton, J.O., Tenore, K.R., Castillejo, F., Schwing, F. B., Atkinson, l. P. and Lavin A. 1987 The relationship of upwelling to mussel production in the rías on the western coast of Spain. Journal of Marine Research 45:, 497-511

Carlson, C. A., Ducklow, H.W. and Michaels, A. F. 1994. Annual flux of dissolved organic carbon from the euphotic zone in the Northwestern Sargasso Sea. Nature, 371:405-408

Carlson C. A. and Ducklow, H.W. 1995. Dissolved organic carbon in the upper ocean of the central equatorial Pacific Ocean, 1992; Daily and finescale vertical variations. Deep-Sea Research II, 42, 2-3: 639-656.

Cauwet, G., Sempere, R. and Saliot, A. 1990 Carbone organique dissous dans l'eau de mer: cofirmation de la sous-estimation antérieure. C.R. Acad. Sci. Paris, 311, Série II: 1061-1066

Cauwet, G. 1994. HTCO method for dissolved organic carbon analysis in seawater: influence of catalyst on blank estimation. Marine Chemistry 47: 55-64.

Culberson, C. H. 1981. Direct potentiometry in marine electrochemistry. In: Whitfield and Jagner. Marine Electrochemistry. J.Wiley and Sons,(editors) Ltd. 522 pp.

Dietrich, G., Kalle, K., Krauss, W. and Siedler, G. 1980. General Oceanography. An Introduction. 2nd Edition. J. Wiley and Sons(editors)., 626 pp.

Doval, M. D., Fraga, F. and Pérez F. F. 1997. Determination of dissolved organic nitrogen in seawater using Kjeldahl digestion after inorganic nitrogen removal. Oceanologica Acta (in press)

Figueiras F.G., Jones K.J., Mosquera A.M., Álvarez-Salgado X.A., Mc Douglas V 1994 Red tide assemblage formation in a estuarine upwelling ecosystem: Ría de Vigo. J. Plankton Res.,16: 857-878

Fraga, F. 1981 Upwelling off the Galician coast, northwest Spain. In: Richards, F. A (editor) Coastal upwelling. Coastal and Estuarine Science, Vol 1, Washington DC: 176-182.

Fraga, F., Pérez F. F., Figueiras F. G. and Ríos, A. F. 1992 Stoichiometric variations of N, P, C and $O_2$ during a Gymnodinium catenatum red tide and their interpretation. Marine Ecology Progress Series 87: 123-134.

Gómez-Fermin. E., Figueiras F. G., Arbones B. and Villarino M. L. 1996. Short-time scale development of a gymnodinium catenatum population in the ría de Vigo (NW Spain). J. Phycol. 32, 212-221

Haynes, R., Barton, E. D. and Pilling I. 1993 Development, persistence and variability of upwelling filaments off the Atlantic coast of the Iberian Peninsula. Journal of Geophysical Research 98 (c12): 22681-22692

Jackson, G., A., 1988. Implications of high dissolved organic matter concentrations for oceanic properties and processes. Oceanogr. 1: 28-33

Kirchman, D. L., Lancelot, C., Fasham, M., Legendre, L., Radach, G. and Scott, M. 1993 Dissolved organic material in biogeochemical models of the ocean. In*:* G. T. Evans & M. J.R. Fasham (editors) Towards a model of Ocean Biogeochemical Processes. Serie I: Global Environmental Change, Vol. 10 Berlin: 209-225

Legendre 1981 Hydrodynamic control of marine phytoplankton production: the paradox of stability, In: Jacques C.J. Nihoul (editor). Ecohydrodynamics. Elsevier Oceanographic Series, 32. Amsterdam 1981: 191-207

López Jamar, E., Cal, R. M., González, G., Hanson, R. B., Rey, J., Santiago, G and Tenore, K. R. 1992 Upwelling and outwelling effects on the benthic regime of the continental shelf off Galicia, NW Spain. J. Mar. Res. 50: 465-488

McClain, C.R., Chao, S.-Y., Atkinson, l. P., Blanton, J.O., and Castillejo, F. 1986. Wind-driven upwelling in the vicinity of Cape Finisterre, Spain, J.Geophys.Res., 91(C7): 8470-8486

Mehrbach, C., Culberson, C.H., Hawley, J.E. and Pytkowicz, R. M. 1973. Measurements of the apparent dissociation constant of carbonic acid in seawater at atmospheric pressure. Limnol. Ocean., 18: 897-907.

Nogueira, E., Pérez F.F. and Ríos, A.F. 1997 Seasonal patterns and long-term trends in an estuarine upwelling ecosystem (Ría de Vigo, NW Spain). Estuarine Coastal Shelf Science, 44: ???-???

Odum, W. E., Fisher, J. S. and Pickral, J. C. 1979. Factors controlling the flux of particulate organic carbon from estuarine wetlands. In: Livingston, R.J (editor) Ecological Processes in Coastal and Marine Systems Plenum Press. New York. : 69-80.

Pérez, F. F., Álvarez-Salgado, X. A., Rosón, G. and Ríos, A.F. 1992. Carbonic-calcium system, nutrients and total organic nitrogen in continental runoff to the Galician Rías Baixas, NW Spain., Oceanologica Acta, 15 (6): 595-602.

Pérez, F. F. and Fraga, F. 1987a. A precise and rapid analytical procedure for alkalinity determination. Mar. Chem., 21:169-182.

Pérez, F. F. and Fraga, F. 1987b The pH measurements in seawater on NBS scale. Mar. Chem., 21: 315-327

Prego, R. and Fraga, F. 1992. A simple model to calculate the residual flows in a Spanish ría. Hydrographic consequences in the ría of Vigo, Estuarine Coastal Shelf Sci., 34: 603-615.

Prego R (1993a). Biogeochemical pathways of phosphate in a Galician Ría (North-Western Iberian peninsula). Estuarine Coastal Shelf Sci., 37: 437-451

Prego R. (1993b). General aspect of carbon biogeochemistry in the ría of Vigo, northwestern Spain. Geochim. Cosmochim. Acta, 57: 2041-2052

Prego, R. 1994 Nitrogen interchanges generated by biogeochemical processes in a Galicia ría. Mar Chem 45: 167-176

Ríos, A. F., Fraga, F. and Pérez, F. F. 1989 Estimation the coefficients for the calculation of ‘NO’, ‘PO’ and ‘CO’, starting from the elemental composition of natural phytoplankton. Scienta Marina 53: 779-784

Ríos, A. F. 1992. El fitoplancton en la Ría de Vigo y sus condiciones ambientales. Ph. D. Thesis, University of Santiago, 416 pp.

Ríos, A. F., Nombela, M.A., Pérez, F. F., Rosón G and Fraga, F. 1992a. Calculation of runoff to an estuary. Ría de Vigo. Scient. Mar., 56(1): 29-33.

Ríos, A. F., Pérez, F. F. and Fraga, F. 1992b. Water masses in upper and middle North Atlantic ocean east of Azores. Deep Sea Res., 39 (3/4): 645-658.

Rosón, G., Pérez, F. F., Álvarez-Salgado, X. A. and Figueiras, F. G. 1995 Variation of both thermohaline and chemical properties in an estuarine upwelling ecosystem: Ría de Arousa. I. Time evolution. Estuarine and Coastal Shelf Science, 41: 195-213

Rosón, G., Álvarez-Salgado, X. A. and Fraga, F. 1997 A non-steady state box model to determine residual flows in a partially mixed estuary based on both thermohaline properties. Estuarine and Coastal Shelf Science, 44: ???-???

Sharp, J. H., Benner, R., Bennett, L., Carlson, C.A., Down, R. and Fitzwater, S. E. 1993. A re-evaluation of high temperature combustion and chemical oxidation measurements of dissolved organic carbon in seawater. Limnol. Oceanogr. 39: 1774-1782.

Takahashi, T., Olafsson J., Goddard J.G., Chipman D. W. and Sutherland S.C. 1993. Seasonal variation of $CO_2$ and nutrients in the high latitude surface oceans: a comparative study. Global Biogeochemical cycles, 7: 843-878

Tenore, K. R. and 14 co-authors 1982 Coastal upwelling in the Rías Baixas, NW Spain. Contrasting the benthic regimes of the Ría de Arousa and Muros. J Mar Res 40: 701-772

Thomas, C., Cauwet, G. and Minster, J.-F. 1995 Dissolved organic carbon in the equatorial Atlantic Ocean. Mar Chem 49: 155-169

Tupas, L. M., Popp, B. N. and Karl, D. M. 1994 Dissolved organic carbon in oligotrophic waters: experiments on sample preservation, storage and analysis. Mar. Chem., 45: 207-216.

UNESCO 1991. Reference Materials for Oceanic Carbon Dioxide Measurements. UNESCO Technical Papers in Marine Science, 60. 41pp

Weiss, R. F. 1974 Carbon dioxide in water and seawater: the solubility of a non-ideal gas. Mar. Chem., 2: 203-215.

Wollast, R., 1991. The coastal organic cycle: fluxes, sources and sinks. In Mantoura R.F.C., Martin M. & Wollast R (editors). Ocean Margin Processes in Global Change. Report of the Dahlem Workshop on Ocean Margin Processes in Global Change, Berlin, March 18-23,1990. Wiley, Chichester: 365-382

Wooster, W. S., Bakun, A. and Mclain, D. R. 1976. The seasonal upwelling cycle along the eastern boundary of the North Atlantic, J. Mar. Res., 34 (2): 131-141

Yentsch, C. S. and Menzel, D.W. 1963. A method for the determination of phytoplankton chlorophyll and phaephytin by fluorescence. Deep-Sea Res., 10: 221-231

**Figure captions**

**Figure 1**. Map of the Ría de Vigo showing the location of sampling stations. The bathymetry , in meters, is also shown

**Figure 2**. Evolution in time of a) Upwelling index (Iw) calculated at 43ºN, 11ºW, b) Runoff estimated as a function of precipitation, c) Incoming solar radiation (Qs) estimated by Mosby´s formula, in the Ría de Vigo from May`94 to September`95.

**Figure 3**. Evolution in time of a) Temperature (ºC), b) Salinity (PSS), c) Nitrate (µmol $kg^{-1}$) and d) Silicate (µmol $kg^{-1}$) distributions in the Ría de Vigo at station **1**, from May`94 to September`95.

**Figure 4**. Evolution in time of a) Temperature (ºC), b) Salinity (PSS), c) Nitrate (µmol $kg^{-1}$) and d) Silicate (µmol $kg^{-1}$) distributions in the Ría de Vigo at station **2**, from May`94 to September`95.

**Figure 5**. Evolution in time of a) Ammonium (µmol $kg^{-1}$) b) Oxygen (µmol $kg^{-1}$), c) $pCO_2$ (µatm) and d) Chlorophyll-*a* (µg $l^{-1}$) distributions in the Ría de Vigo at station **1**, from May`94 to September`95.

**Figure 6**. Evolution in time of a) Ammonium (µmol $kg^{-1}$) b) Oxygen (µmol $kg^{-1}$), c) $pCO_2$ (µatm) and d) Chlorophyll-*a* (µg $l^{-1}$) distributions in the Ría de Vigo at station **2**, from May`94 to September`95

**Figure 7** Temperature-Salinity diagram for maximum salinity samples on every surveys at station **1** and **2** and ENAW line.

**Figure 8**. Dissolved Organic Carbon (DOC, µM) distribution at stations **1** (a) and **2** (b) during the sampling period.

Table 1. Sampling dates of Radial transects, grouped following the wind-featured seasons

| **Upwelling season ´94** | | **Non-upwelling season ´94-´95** | | **Upwelling season ´95** | |
|---|---|---|---|---|---|
| RADIAL | DATE | RADIAL | DATE | RADIAL | DATE |
| 1 | May, 5 | 13 | November, 4, 1994 | 21 | March, 1 |
| 2 | May, 26 | 14 | November, 16, 1994 | 22 | March, 23 |
| 3 | June, 9 | 15 | December, 1, 1994 | 23 | April, 6 |
| 4 | June, 23 | 16 | December, 22, 1994 | 24 | April, 20 |
| 5 | July, 6 | 17 | January, 12, 1995 | 25 | May, 11 |
| 6 | July, 21 | 18 | January, 26, 1995 | 26 | May, 25 |
| 7 | August, 4 | 19 | February, 9, 1995 | 27 | June, 8 |
| 8 | September, 1 | 20 | February, 23, 1995 | 28 | June, 22 |
| 9 | September, 8 | | | 29 | July, 6 |
| 10 | September, 29 | | | 30 | July, 20 |
| 11 | October, 6 | | | 31 | August, 3 |
| 12 | October, 20 | | | 32 | August, 24 |
| | | | | 33 | September, 8 |
| | | | | 34 | September, 21 |

Table 2.- Statistics of the daily cross-shore Ekman transport time series during the analysed period. Data are grouped according to the astronomic and the wind-featured seasons. The number of data (n), mean value, standard deviation (sd), coefficient of variation (CV), lower and upper quartiles and the observed periodicities (ordered by the ammount of variance they retain), are shown.

| **season** | | **n** | **mean** | **sd** | **CV (%)** | **25 th** | **75 th** | **period (days)** |
|---|---|---|---|---|---|---|---|---|
| astromomic | | | | | | | | |
| | summer ‘94 | 92 | 350 | 607 | 173 | 19 | 566 | 7, 12, 30 |
| | fall ‘94 | 91 | –110 | 945 | 833 | –349 | 222 | 30, 10, 2 |
| | winter ‘94-’95 | 90 | –803 | 1455 | 181 | –1458 | 193 | 22, 2-7 |
| | spring ‘95 | 92 | 198 | 968 | 500 | –101 | 683 | 11, 4 |
| | summer ‘95 | 92 | 546 | 674 | 123 | 93 | 879 | 7, 14 |
| wind-featured | | | | | | | | |
| | upwelling ‘94 | 184 | 188 | 651 | 346 | –108 | 484 | 7, 10, 40 |
| | downwelling ‘94-’95 | 150 | –533 | 1370 | 257 | –1022 | 220 | 24, 3 |
| | upwelling ‘95 | 184 | 355 | 853 | 240 | 26 | 764 | 3-10, 26, 50 |

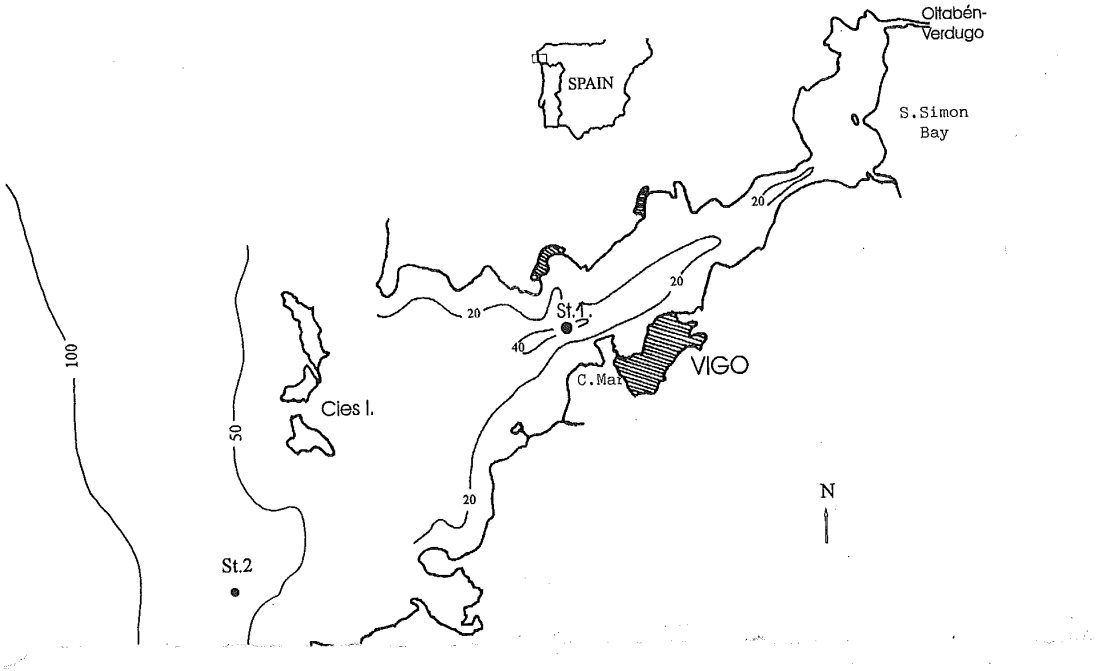


(Fig 1. Doval et al)

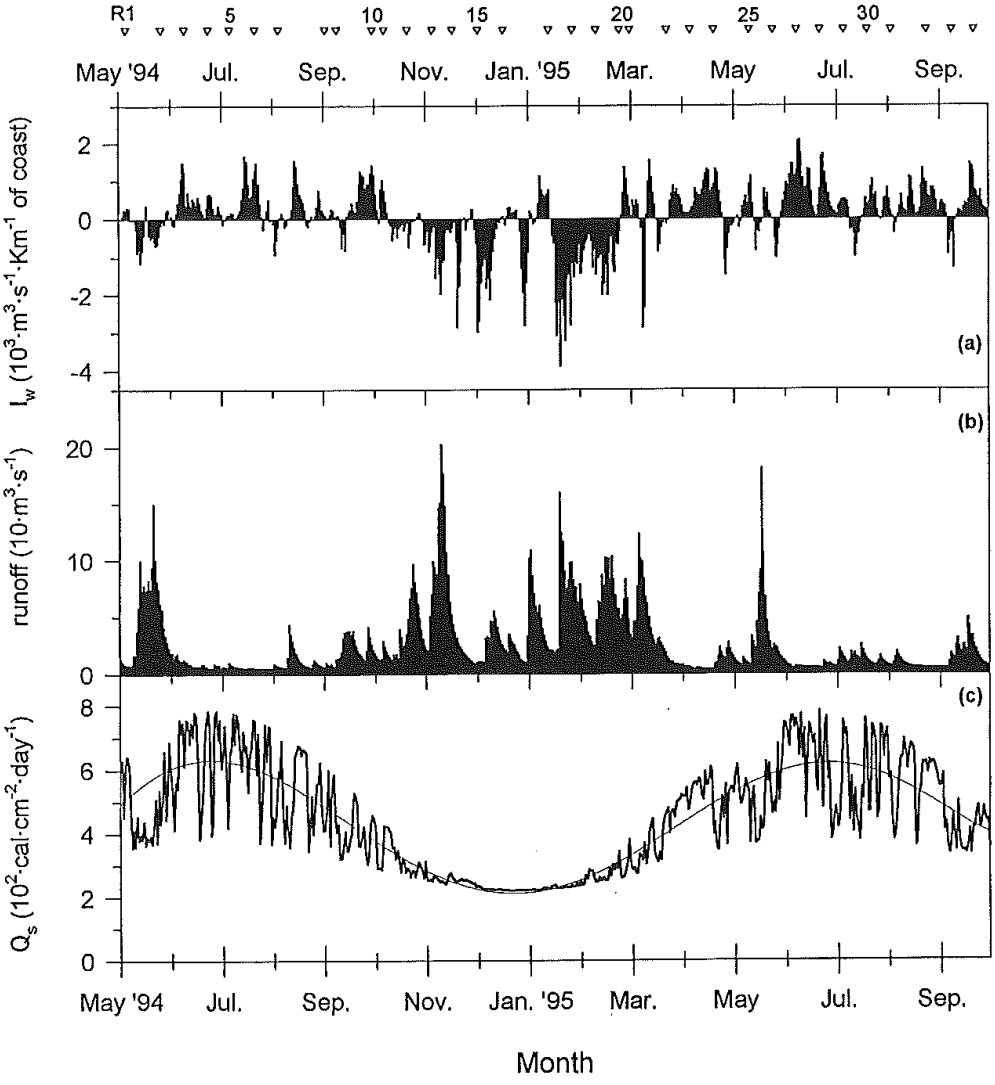


Fig.2. (Doval et al.,)

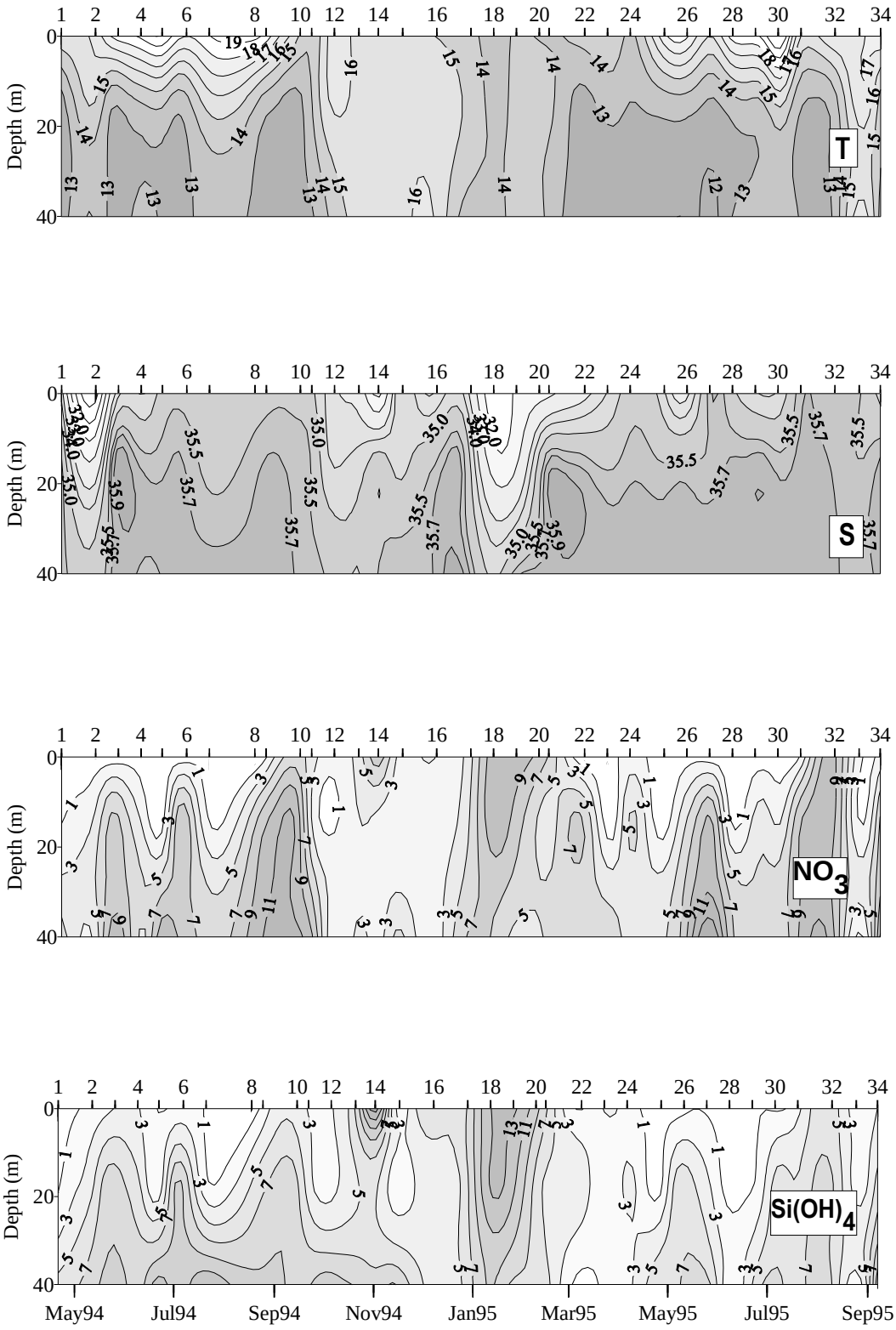


Fig.3. (Doval et al.,)

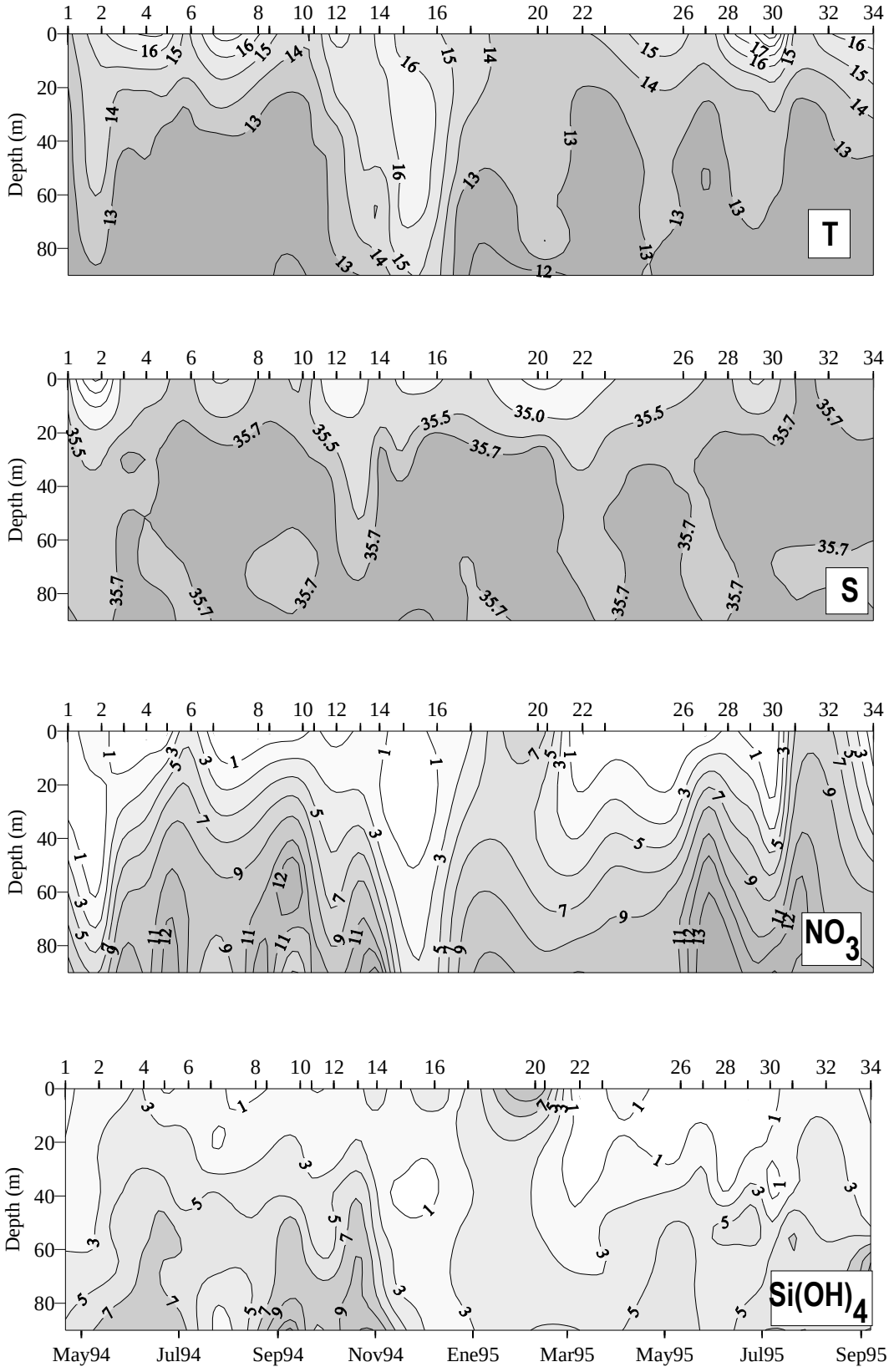


Fig.4. (Doval at al.,)

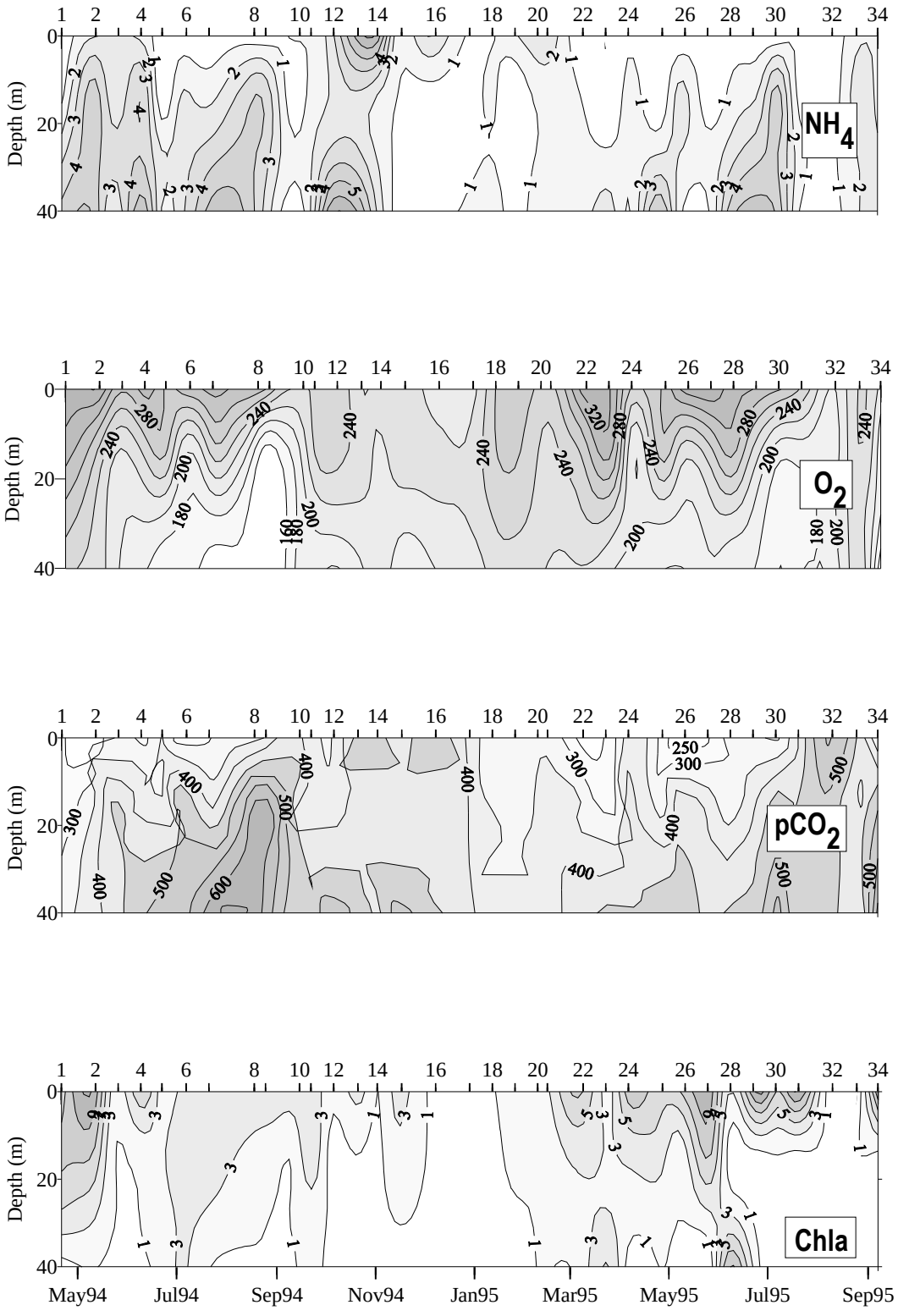


Fig. 5 (Doval at al.,)

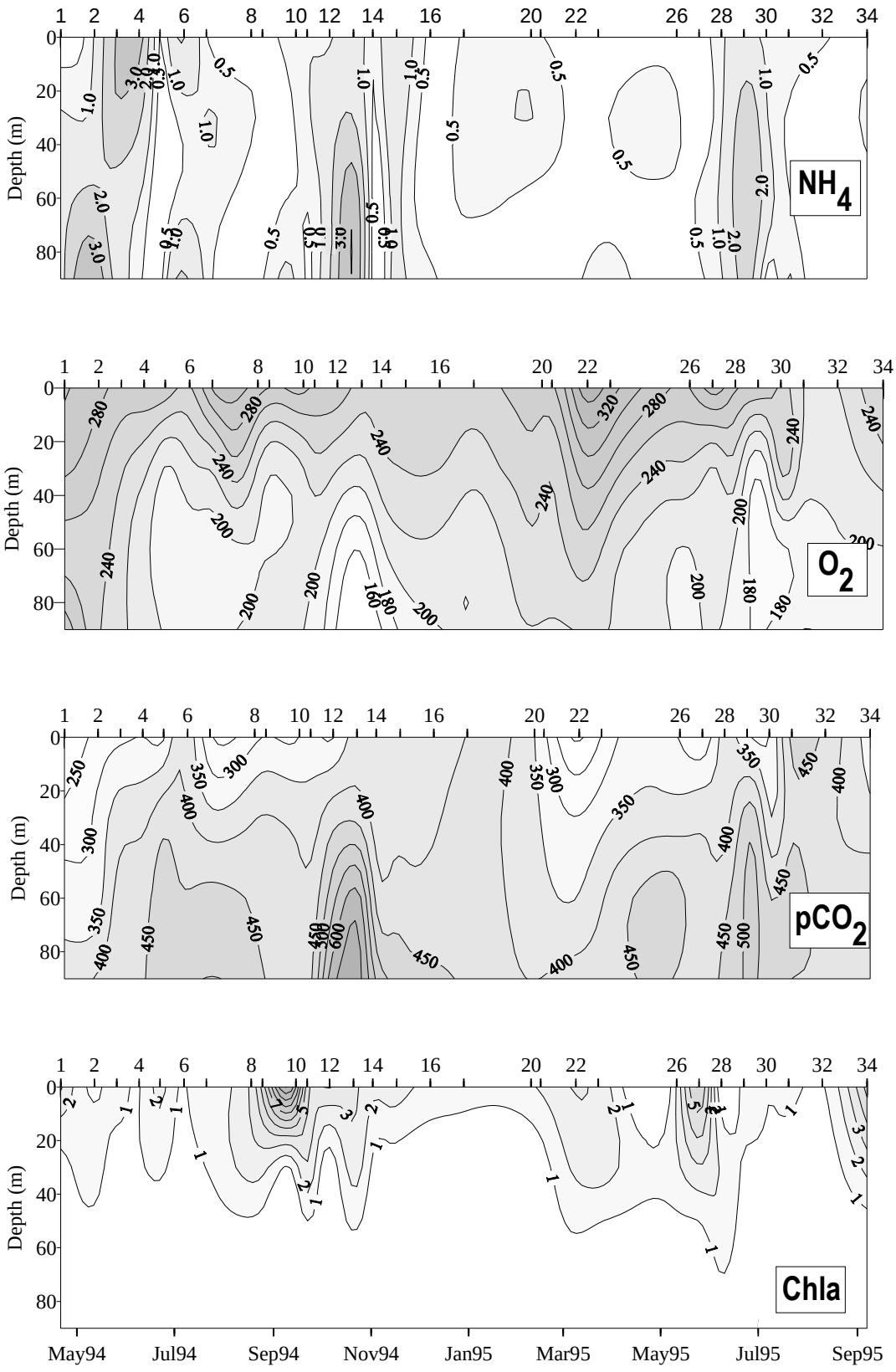


Fig. 6 (Doval at al.,)

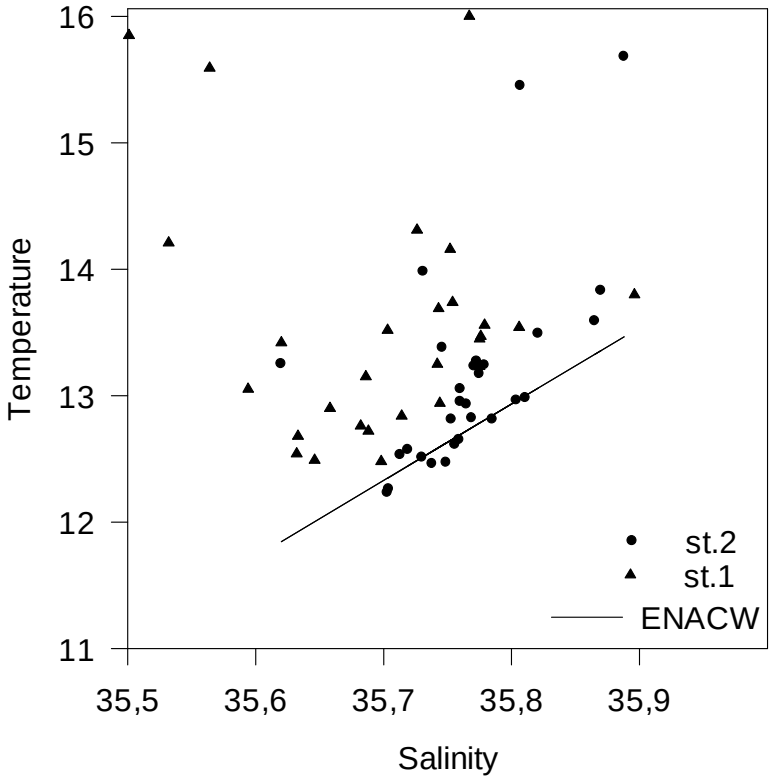


Fig 7. (Doval at al.,)

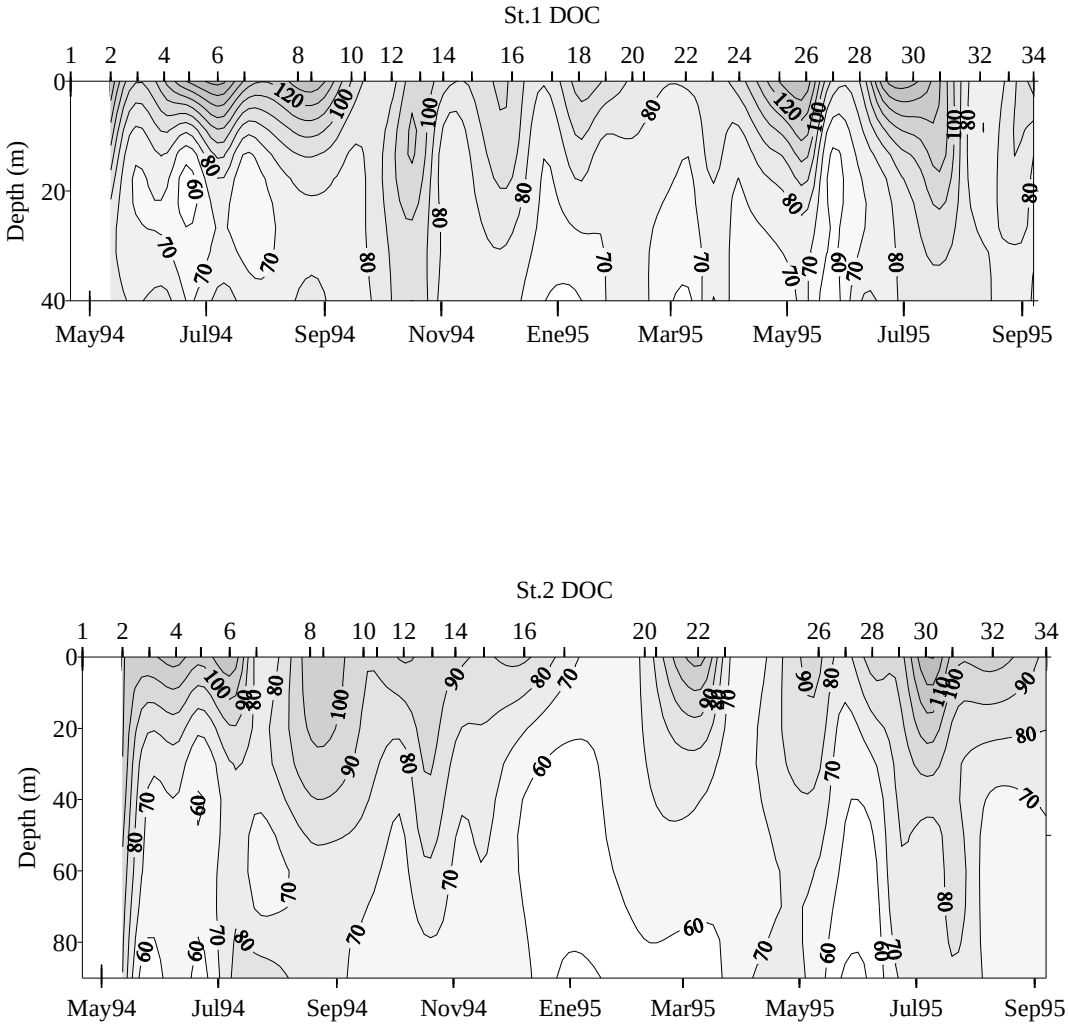


Fig. 8 (Doval et al.,)